# Development of a Modified Flat-plate Test Specimen and Fixture for Composite Materials Crush Energy Absorption

PAOLO FERABOLI*

*Department of Aeronautics and Astronautics, University of Washington*
*Seattle, WA, USA*

**ABSTRACT:** There are currently no specialized test methods for the characterization of specific energy absorption (SEA) of composite materials. Based on an original concept developed by NASA in the early 1990s, a test method that utilizes a flat plate-like specimen and a modified anti-buckling fixture is presented here that introduces a region of unsupported material in the proximity of the crush front, and allows the specimen to deform freely. A systematic experimental investigation is conducted with two unidirectional tapes to verify the general applicability of the test method to screen candidate material systems, and to isolate the effect of the unsupported distance on the measured SEA values. In general, it is found that there are four failure mechanisms (fragmentation, frond formation, local, and global buckling) that compete as the dominating mode according to the chosen unsupported distance. The specimen and fixture combination presents several limitations, but with a properly selected unsupported distance it could be used to assess the SEA of material and structures whose dominating failure mechanism is frond formation.

**KEY WORDS:** crashworthiness, energy absorption, test standard.

## INTRODUCTION

THE FOUR NECESSARY conditions for survival during a vehicle collision are maintaining sufficient occupant space, providing adequate occupant restraint, employing energy-absorbing devices, and allowing for a safe post-crash egress from the craft [1]. In general, while the total energy dissipated during a crash depends on the overall vehicle system deformation, the crash-oriented design of the individual structural subcomponents of simple geometry can provide a great increase in structural crashworthiness and survivability, with an acceptable increase in overall vehicle cost. For this reason, structural elements that provide energy absorption have received special attention in the literature [2–6].

Energy absorbers can be found in the front end of all modern passenger cars in the form of collapsible tubular rails [4, 5]. In addition, collapsible floor stanchions and beams are now finding their way into modern aircraft keel structures [6–9].

These elements have been traditionally made of steel or aluminum, which absorb energy through controlled collapse by folding and hinging, involving extensive local plastic deformation. However, the introduction of composites in the primary structure of modern air- and ground-vehicles presents special problems for the designer dealing with occupant safety and crashworthiness. The energy-absorbing behavior of composites is not easily predicted due to the complexity of the failure mechanisms that can occur within the material. Composite structures fail through a combination of fracture mechanisms. These involve a complex series of fiber fracture, matrix cracking, fiber-matrix debonding, and interlaminar damage (delamination) mechanisms. The brittle failure modes of many polymeric composite materials can make the design of energy-absorbing crushable structures difficult. Furthermore, the overall response is highly dependent on a number of parameters, including the geometry of the structure, material system, lay-up, and impact velocity.

The vast majority of the work in the area of crashworthiness energy absorption has focused on thin-wall tubular specimens [2–6]. Only a very limited number of attempts have been made at developing a flat-plate-shaped specimen to determine the energy absorption of composite materials. The following paragraphs review in detail the advantages and shortcomings of each test method in order to introduce the proposed test method.

## REVIEW OF THREE RELEVANT PREVIOUS FIXTURES

The Army Research Laboratories (ARL) in conjunction with Virginia Tech performed pioneering work done in the early 1990s at NASA Langley Research Center [10–13], and set the basis for most of the future evolutions of flat plate specimen fixtures [14–16]. The NASA group proposed a test method featuring a flat-plate rectangular specimen and a dedicated test fixture designed to provide anti-buckling stability during crushing (Figure 1). Lateral support to the specimen is provided through knife-edges, which fit into a set of four inner vertical posts. Four vertical guide rods with linear roller bearings are used to provide support to the upper plate sliding relative to the lower plate, and a steel sphere is used to ensure full alignment of the loading cross-head with respect to the fixed base. Two specimen sizes and relative fixtures, scaled geometrically by a factor of two, were considered and compared, and are shown in Figures 1 and 2. The fixture was set for a specific laminate thickness and specimen width, and evaluation of different thicknesses was not allowed without rebuilding a scaled fixture. For the specimen, two types of trigger mechanisms, the so-called 'steeple' (a double chamfer) and 'notch' (a staggered, transverse machined profile) were employed, and are shown in Figure 2. It was reported [10] that the steeple trigger had a tendency to generate a double peak in the initial portion of the load–stroke diagram, possibly due to the formation of a long delamination along the length of the specimen. The 45° chamfered trigger, commonly used in tubular specimens, was not employed because it could not produce a well-defined peak load prior to dropping to a sustained crushing load. With the aforementioned exceptions, the researchers successfully achieved sustained crushing both in quasi-static and dynamic test conditions, although in the latter case, they required the use of pulse-shaping devices to avoid undesired oscillations due to the indirect impact on the steel fixture.
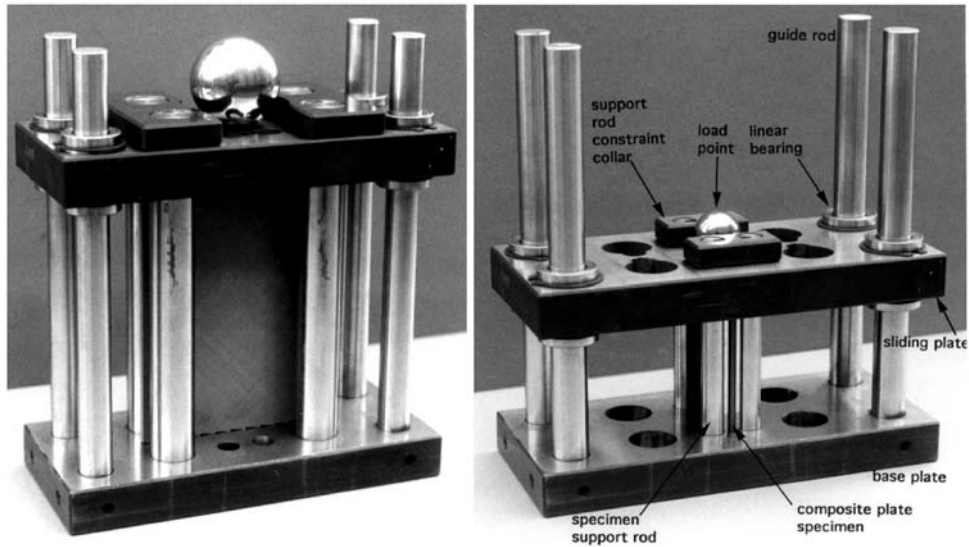
**Figure 1.** *Test fixture and specimen developed by NASA [10–12].*
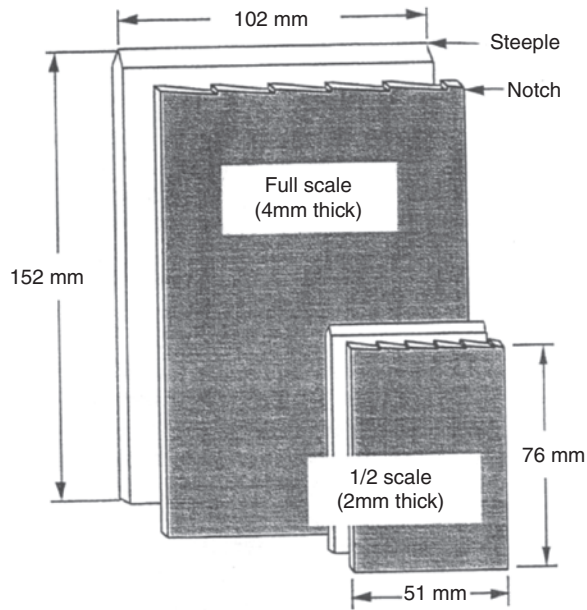


**Figure 2.** *Test specimen used by NASA, featuring notch and steeple triggers.*

However, although the fixture yielded force–stroke traces that closely resembled those of tubular specimens, the SEA values obtained with this method did not compare well with others previously obtained [3] by testing thin-wall tubular specimens of the same material systems and laminate designs.

In an effort to understand the validity of the proposed flat-plate specimen, Bolukbasi and Laananen [17] conducted a systematic comparison of three structural configurations.

Flat plates, angle sections, and C-channels manufactured with identical materials, lay-ups, and crush initiators were crushed under quasi-static conditions (Figure 3). Although the number of specimens tested was limited, as was the selection of laminate lay-ups, it was found that the flat plates tested with the NASA fixture yielded higher SEA measurements than any of the self-supporting specimens, mostly attributable to the overly constrained nature of the specimen.

In recent years, a modification to the NASA fixture was suggested [14,15], which could accommodate for variable specimen width and thickness by introducing adjustable knife-edge supports (Figures 4(a), (b)). These were tightened only to the minimum necessary to maintain contact with the specimen but minimize friction. The trigger used was a 45° steeple, identical to the NASA one. While the detailed geometry of the fixture significantly changed, the overall philosophy and mechanics of deformation remained unchanged with respect to the NASA fixture. The knife-edges, while preventing the plate from buckling, also promoted local tearing of the laminate (Figure 5) at the supports, similar to the failure modes observed with the NASA fixture. This characteristic of the fixture, besides potentially absorbing large amounts of energy and possibly leading to unrealistic SEA values, had the potential to significantly affect the crush progression of the specimen by favoring a certain failure morphology over others.

A further evolution of the NASA fixture was shown by Engenuity [16] in limited detail. The fixture consisted of a rig that provides anti-buckling stability by fully constraining lateral and out-of-plane movement of the coupon, while at the same time enabling it to deform freely in the proximity of the crush front (Figure 6). The specimen featured a trigger
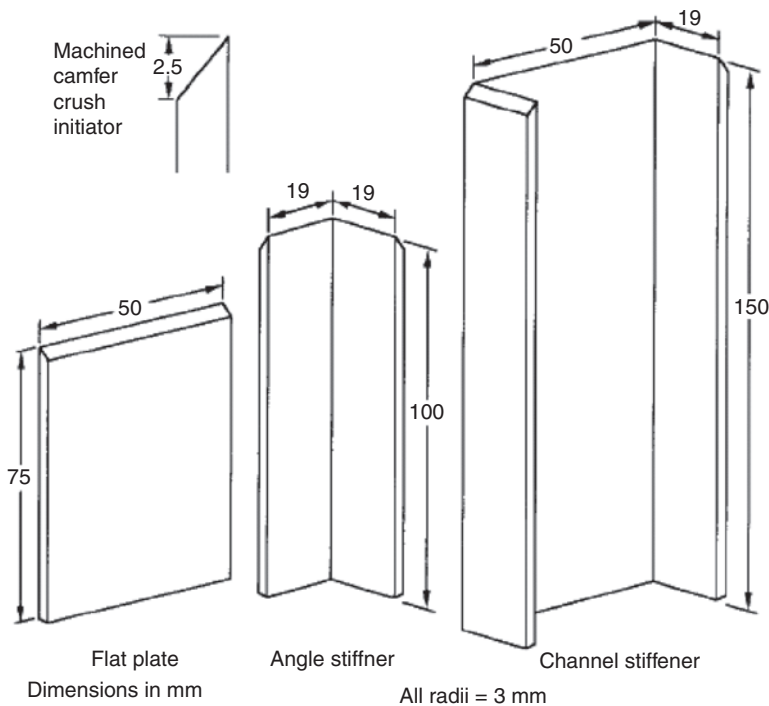


**Figure 3.** *Systematic comparison of specimen geometry on the measured SEA [17], and associated average SEA values in J/g for two stacking sequences.*
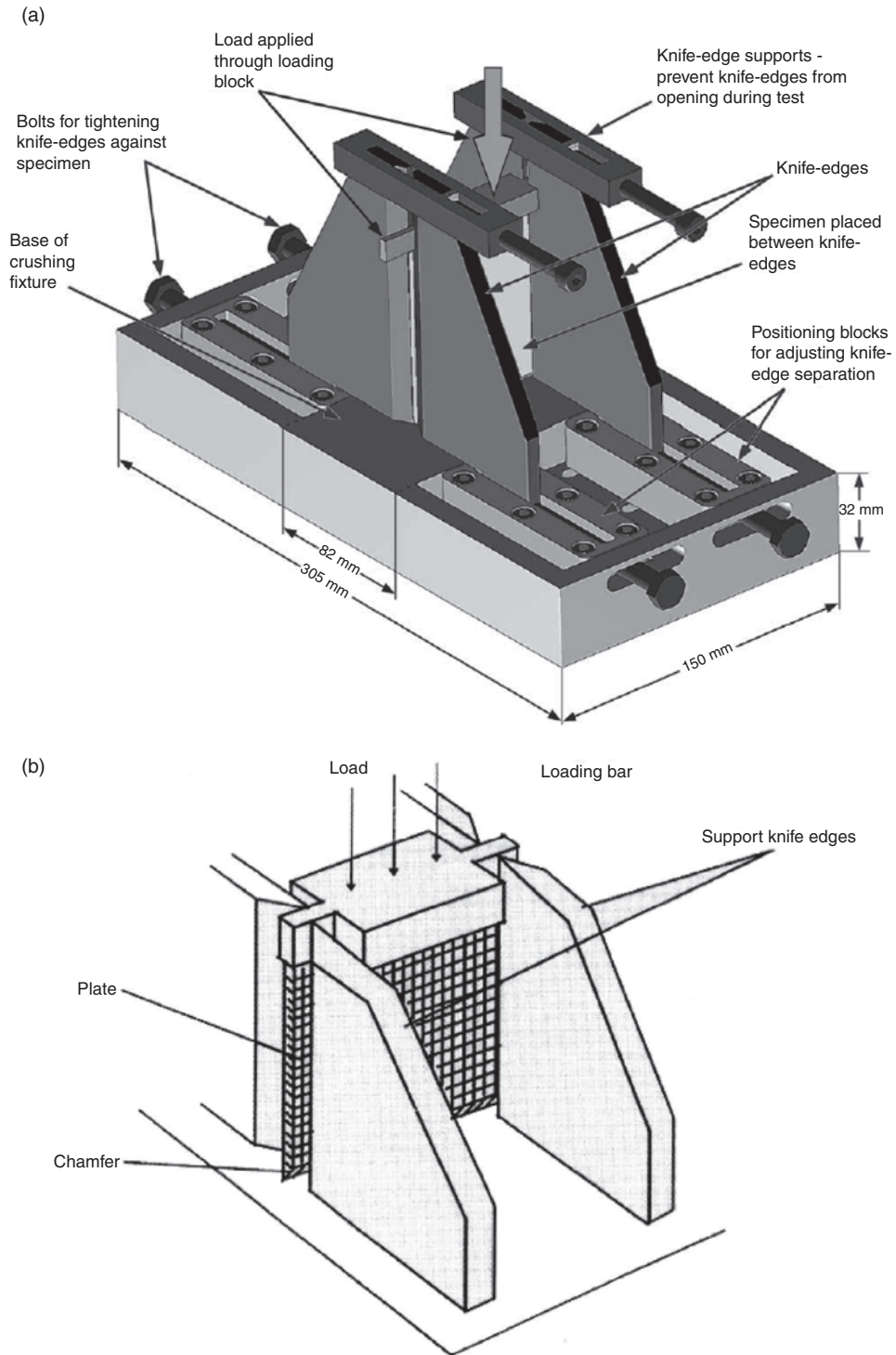
(a)

Load applied through loading block

Knife-edge supports - prevent knife-edges from opening during test

Bolts for tightening knife-edges against specimen

Knife-edges

Base of crushing fixture

Specimen placed between knife-edges

Positioning blocks for adjusting knife-edge separation

32 mm

82 mm

305 mm

150 mm

(b)

Load

Loading bar

Support knife edges

Plate

Chamfer

**Figure 4.** *(a, b) Detailed and symbolic representation of the test fixture developed in [14,15].*
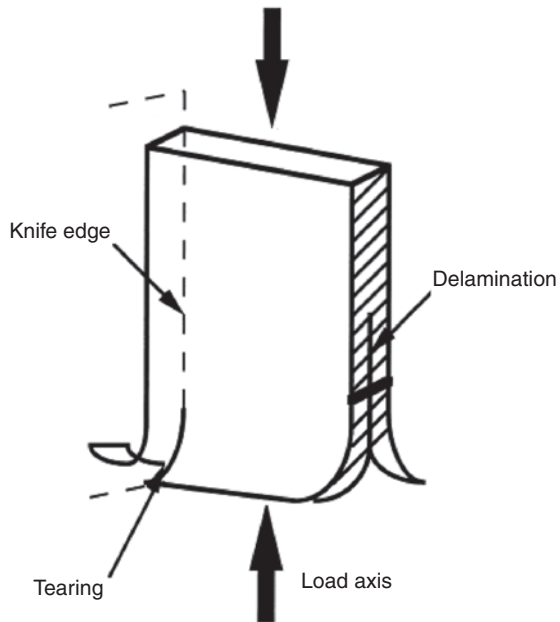
**Figure 5.** *Undesirable characteristic of this set-up is the tearing at the supports, which produces unrealistic SEA values [10–12,14,15].*
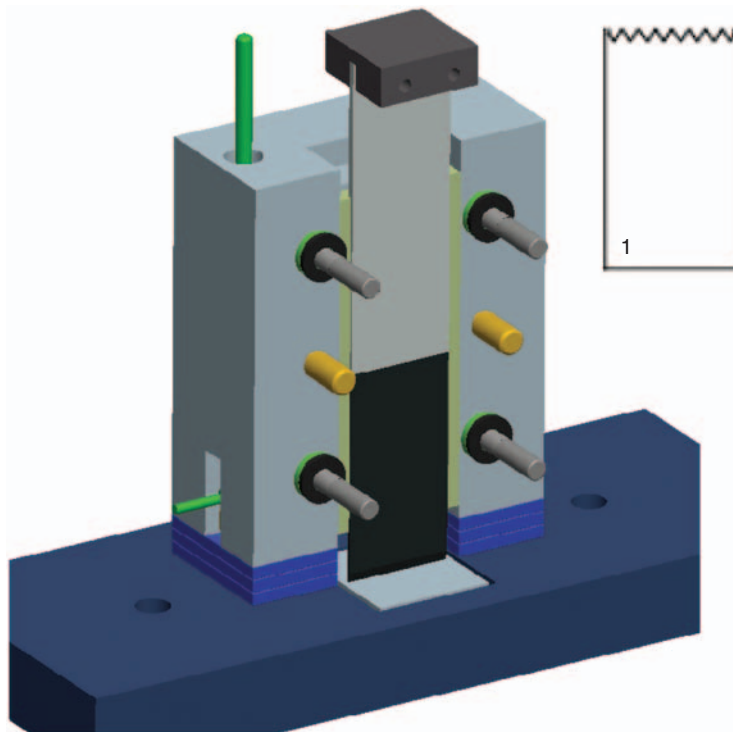


**Figure 6.** *Test fixture and specimen (with saw-tooth trigger) developed in [16].*

with a planar saw-tooth shape (Figure 6), similar to the notch trigger used by NASA. As all other triggers, whether planar or tapered in the thickness direction, it favors the progressive load introduction in the coupon through its reduced section area. The fixture comprises low-friction polymeric supports on the surfaces contacting the specimen, and can partially accommodate specimens of varying thickness by using shims. The most significant difference between this fixture and the NASA fixture is that the specimen is here allowed to deform freely in proximity of the crush front. The unsupported distance between the specimen supports and the base-plate, which is varied by introducing spacer blocks of various heights, allows the material to crush in an unconstrained fashion. The researchers have shown that materials tend to behave more or less favorably depending on the value of the 'spacer height', hence the value of this unsupported distance appears to have an effect on the measured SEA [16]. Overall, while allowing the specimen to deform more naturally, the unsupported distance adds further complexity to the fixture by introducing a new variable. In this work, an attempt is made to introduce an unsupported distance in the original NASA fixture, while systematically characterizing its effects on the SEA measurements.

## EXPERIMENTAL SETUP

Two material systems were supplied by Toray Composites of America:

A. unidirectional tape prepreg using a T700 fiber, and a 270°F cure resin (132°C), and

B. unidirectional tape prepreg using a T800 fiber and a 350°F (177°C) highly toughened curing resin.

For all materials, the lay-up considered is $[0/90]_{3s}$, yielding an average cured laminate thickness of 0.079 in. (2.0 mm). The flat coupon is 3.0 in. long (76.2 mm) and 2.0 in. wide (50.80 mm), identical to the original NASA specimen. Two types of triggers are investigated, the 45° steeple used by NASA [10–12] and the saw-tooth [17], both shown in Figure 7.

The fixture developed for this investigation (Figures 8–11) builds upon the NASA fixture, employing knife-edge supports, and features adjustable screw-driven support plates, which are essentially the ones used in [14]. This feature allows for specimens of different thickness to be tested without shims. A close-up view from above of the knife-edges is shown in Figure 10. The region of unsupported specimen height, which is defined by the distance between the end of the knife-edge supports and the contact point between the specimen and the base plate, is shown in Figure 11. The modified fixture enables the specimen to deform in a natural fashion by allowing the fronds to bend freely, and also prevents accumulation of a debris wedge between the knife-edges. The unsupported distance can be varied between 0 and 1 in. (0 and 25.4 mm respectively), with intermediate values at 0.125, 0.25, 0.5, and 0.75 inches (3.2, 6.3, 12.7, 19.0, and 25.4 mm), and is achieved by moving the two sets of knife-edges up or down from the base-plate. For 0 in. (0 mm) unsupported height, the fixture is virtually equivalent to the original NASA fixture, thus providing a fully constrained specimen.

Knife-edges are positioned in contact with the specimen manually, and the degree of constraint is arbitrarily defined as finger-tight. It is a compromise between excessive clamping, which increases friction and hence energy absorption, and inefficient clamping, which then leads to unstable crushing and favors premature buckling.

Similar to the NASA fixture, the loading plate is free to slide along four vertical posts, which use roller bearings for alignment and reduced friction. A self-aligning sphere is used to introduce the load from the test frame onto the loading plate. All tests are conducted at
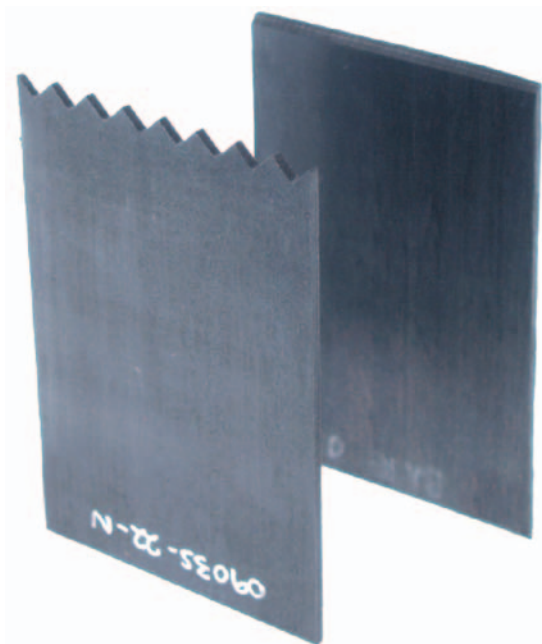
**Figure 7.** *Saw-tooth and steeple trigger specimens used in this investigation.*
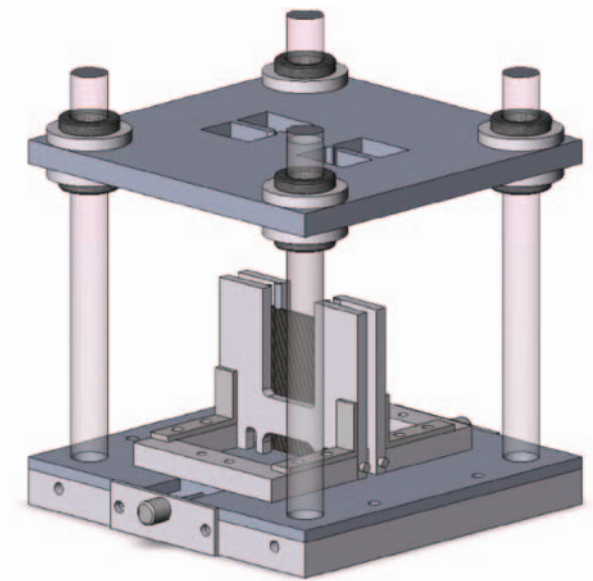


**Figure 8.** *View of proposed fixture for flat specimens, showing 0-in. (0 mm) unsupported height.*

a quasi-static rate of 2.0 in./min (50.8 mm/min), which is noticeably below any dynamic effect previously reported for modern systems [5], usually around 40 in./s (1 m/s). Specimens rest on a polished hardened steel surface. For each unsupported distance, a minimum of three and up to five specimens are tested for repeatability.
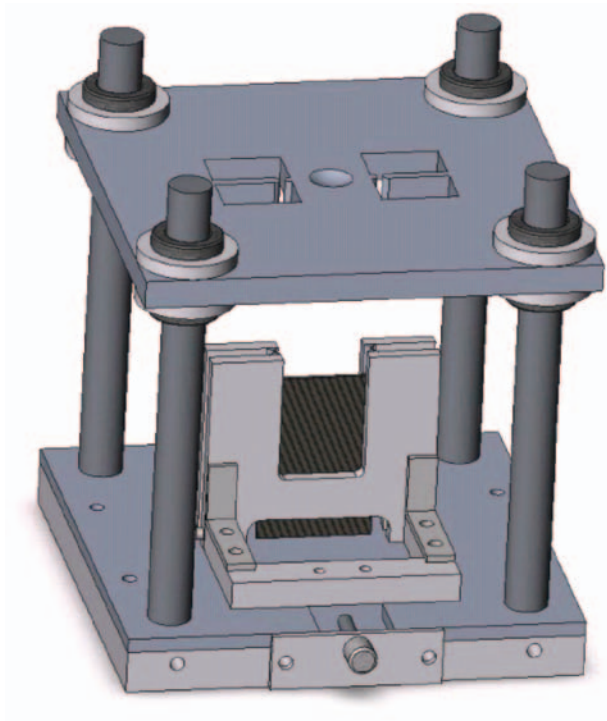
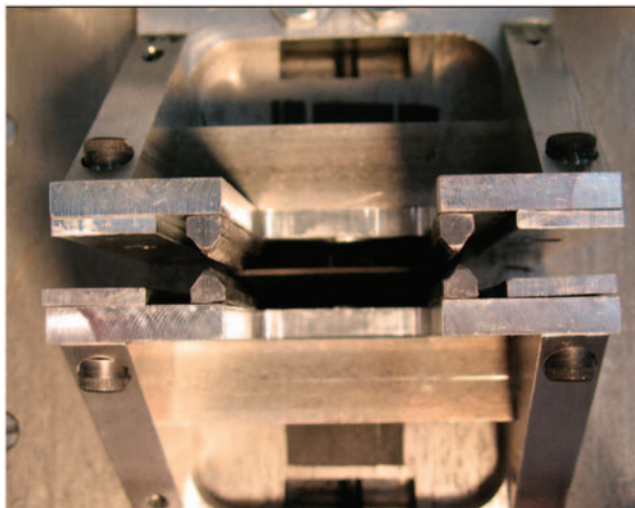**Figure 9.** *Another view of proposed fixture for flat specimens, showing 0.25-in. (6.3 mm) unsupported height.*



**Figure 10.** *Top view of the knife-edges supporting the specimen.*

## RESULTS

As expected, the unsupported height has great influence over the measured SEA, as do trigger shape and material type. This section therefore first addresses the characteristic
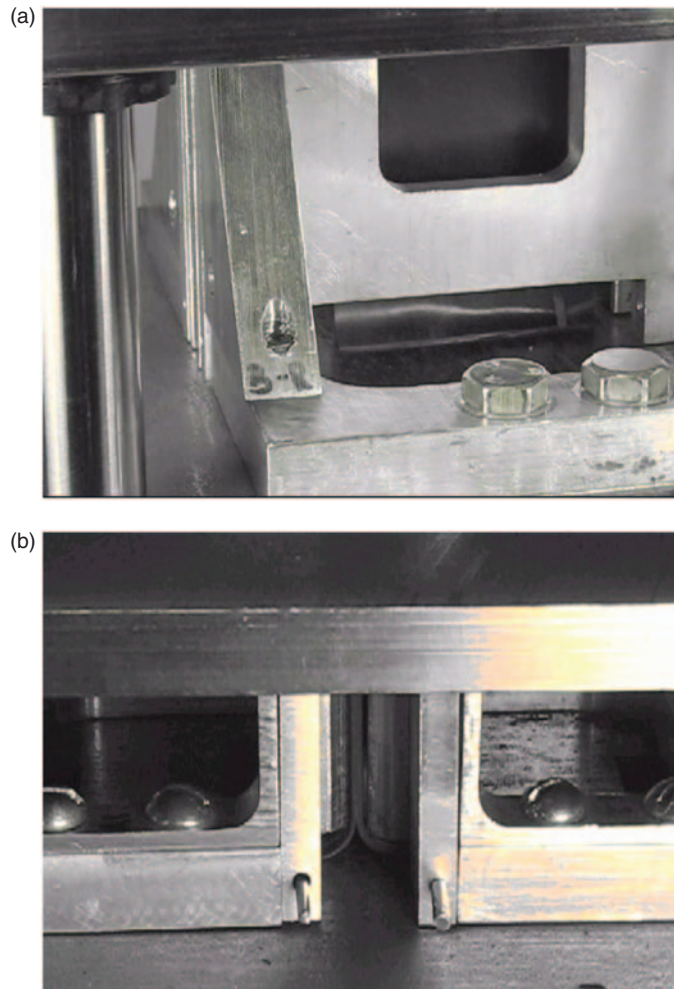
**Figure 11.** View of specimen positioned in the fixture with 0.2 in. (6.3 mm) unsupported height, showing ability of specimen to deform unconstrained.

results observed for material A, and then proceeds to report the observed trends for material B (toughened). For each family of specimens tested, Table 1 summarizes the average SEA over five specimens tested, and the failure mechanism associated with it. Table 2 summarizes the quantities used in this study; in particular, it reports the methodology used to obtain plots such as the one of Figure 12. Normalized load is obtained by dividing the instantaneous value by the maximum value of load achieved during the test. Total energy is calculated by integrating the load vs. deflection curve using the trapezoidal rule, and then normalized by dividing the instantaneous value by the maximum value of energy absorbed achieved during the test. Specific energy absorption (SEA) is calculated by dividing the total energy by the mass of the crushed specimen, which is in turn given by the product of density ($\rho$), thickness ($t$), width ($w$), and stroke ($D$). It is subsequently normalized by dividing the instantaneous value by the maximum value of SEA achieved during the test.

*Table 1. Variables considered in the design of experiment for this study.*

| Material | Unsupported height (in.) | Trigger | Average SEA (J/g) | Failure mode |
|---|---|---|---|---|
| A | 0.000 | Steeple | 29 | Fragmentation + frond formation + tearing |
| A | 0.000 | Saw-tooth | 35 | Fragmentation + frond formation + tearing |
| A | 0.125 | Steeple | 5 | Frond formation |
| A | 0.125 | Saw-tooth | 8 | Frond formation |
| A | 0.250 | Steeple | 4 | Frond formation |
| A | 0.250 | Saw-tooth | 4 | Frond formation |
| A | 0.500 | Steeple | 4 | Frond formation |
| A | 0.500 | Saw-tooth | 7 | Frond formation |
| A | 0.750 | Steeple | 4 | Frond formation |
| A | 0.750 | Saw-tooth | 6 | Frond formation |
| A | 1.000 | Steeple | 4 | Frond formation |
| A | 1.000 | Saw-tooth | 4 | Frond formation |
| B | 0.000 | Steeple | 64 | Fragmentation + frond formation + tearing |
| B | 0.000 | Saw-tooth | 83 | Fragmentation + frond formation + tearing |
| B | 0.125 | Steeple | 44 | Frond formation |
| B | 0.125 | Saw-tooth | 64 | Frond formation |
| B | 0.250 | Steeple | 37 | Frond formation |
| B | 0.250 | Saw-tooth | 60 | Frond formation |
| B | 0.500 | Steeple | 32 | Frond formation |
| B | 0.500 | Saw-tooth | 61 | Frond formation |
| B | 0.750 | Steeple | 20 | Large folding/buckling |
| B | 0.750 | Saw-tooth | 28 | Large folding/buckling |
| B | 1.000 | Steeple | 23 | Large folding/buckling |
| B | 1.000 | Saw-tooth | 25 | Large folding/buckling |

## Material A

For 0 in. (0 mm) unsupported distance, hence, with the specimen fully constrained by the knife-edges in a fashion identical to the NASA fixture [10–12], the specimens of material A crush in a stable manner, as shown in Figure 12, which plots the normalized values of load, total energy, and SEA against stroke. The load curve exhibits a large initial spike, and then levels stably around 50% of the max value. Several highs and lows can be seen, giving rise to a relatively jagged curve, but overall the crush is progressive and stable, as shown by the energy curve, which is nearly perfectly linear, and the SEA curve, which also quickly reaches a nearly constant value. These curves are in many ways similar to those obtained by crushing tubular specimens [3,6] and corrugated specimens [18], and hence were initially considered desirable by the NASA investigators. The overall failure mode is a mixture of frond formation of the outer zero ply, and fragmentation of the remaining plies in the interior of the laminate. However, the same limitations for the 0 in. (0 mm) setup that were mentioned in the literature review are here confirmed. Inspection of the failed specimens reveals that the outermost portions of the laminate (Figure 13(a) and (b)), outside the knife-edges, remain intact as they undergo tearing from the rest of the specimen. This failure mode absorbs an unknown amount of energy. Furthermore, delamination propagation and frond formation are suppressed in favor of a fragmentation crushing mode, thus giving rise to a mixed failure mode.

**Table 2. Summary of methods of calculation of key quantities used in the study.**

| Load (N) | Normalized load (−) | Stroke (cm) | Energy (J) | Total energy (J) | Normalized total energy (−) | SEA (J/g) | Normalized SEA (−) |
|---|---|---|---|---|---|---|---|
| $L_1$ | $L_1/\max{(L_1:L_N)}$ | $D_1$ | $E_1 = 0$ | $EA_1 = 0$ | $EA_1/\max{(EA_1:EA_N)}$ | $SEA_1 = EA_1/(\rho * t * w * D_1)$ | $SEA_1/\max{(SEA_1:SEA_N)}$ |
| $L_2$ | $L_2/\max{(L_1:L_N)}$ | $D_2$ | $E_2 = (D_2 - D_1) * (L_2 + L_1)/2$ | $EA_2 = EA_1 + E_2$ | $EA_2/\max{(EA_1:EA_N)}$ | $SEA_2 = EA_2/(\rho * t * w * D_2)$ | $SEA_2/\max{(SEA_2:SEA_N)}$ |
| $L_3$ | $L_3/\max{(L_1:L_N)}$ | $D_3$ | $E_3 = (D_3 - D_2) * (L_2 + L_1)/2$ | $EA_3 = EA_2 + E_3$ | $EA_3/\max{(EA_1:EA_N)}$ | $SEA_3 = EA_3/(\rho * t * w * D_3)$ | $SEA_3/\max{(SEA_3:SEA_N)}$ |
| $\vdots$ | $\vdots$ | $\vdots$ | $\vdots$ | $\vdots$ | $\vdots$ | $\vdots$ | $\vdots$ |
| $L_N$ | $L_N/\max{(L_1:L_N)}$ | $D_N$ | $E_N = (D_N - D_{N-1}) * (L_N + L_{N-1})/2$ | $EA_N = EA_{N-1} + E_N$ | $EA_N/\max{(EA_1:EA_N)}$ | $SEA_N = EA_N/(\rho * t * w * D_N)$ | $SEA_N/\max{(SEA_1:SEA_N)}$ |
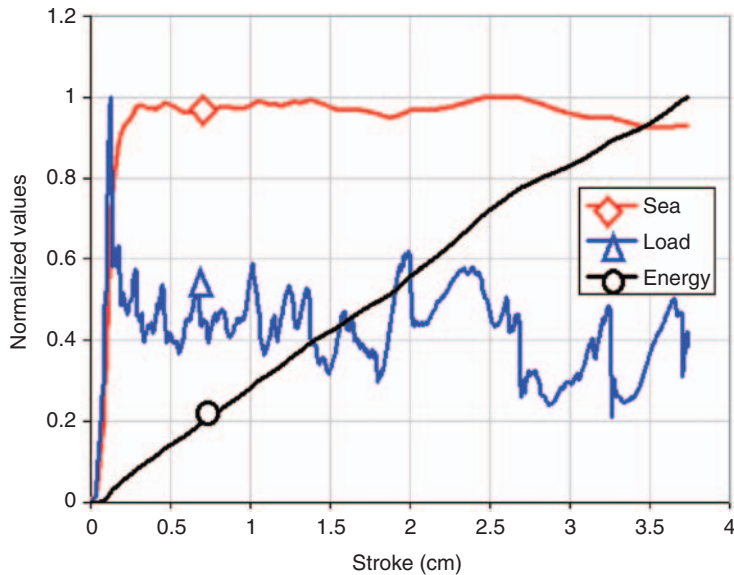
**Figure 12.** *Load, SEA, and total energy absorbed vs. stroke at 0 in. unsupported height (same as original NASA), material A, and notch or steeple trigger.*

Varying the unsupported height to 0.125 in. (3.2 mm) or higher dramatically changes the observed behavior. The load, energy, and SEA curves are plotted vs. stroke in Figure 14. The load curve shows an initial peak, corresponding to the triggering of the crush, and a sudden drop to a virtually zero load value. The EA curve clearly shows that after the initial triggering and formation of a delamination front at the mid-plane of the laminate, its slope dramatically reduces to a nearly horizontal line. The low energy absorption, constant throughout the remaining portion of the test, is due to the propagation of the delamination front. The SEA curve shows a progressive drop in value from the one measured right after triggering, and tends to reach an asymptotic zero value.

Unlike the case of the 0 in. (0 mm) support, for material A (untoughened) the failure mode radically changes to pure delamination propagation (Figure 15(a) and (b)), while fragmentation never occurs. This failure mechanism absorbs less energy than the previous one, as shown in Figure 16, which plots the measured SEA as a function of unsupported height. For this relatively brittle material, the SEA remains constant around 5–10 J/g in the entire range of unsupported distance between 0.125 and 1.0 in. (3.2 and 25.4 mm).The delamination propagates along the mid-plane until it reaches the portion of the laminate in contact with the knife-edges, which act to suppress the delamination. The higher the unsupported distance, the longer the delamination front.

It should be noted that for material A, the sawtooth trigger seems to yield slightly higher values of SEA for the 0 in. (0 mm) unsupported height, see Table 1, but overall the effects on crush energy and failure morphology do not appear to be very noticeable (Figure 16).

**Material B**

Material B behaves relatively similar to material A for the 0 in. (0 mm) unsupported distance. Specimens crush in a stable manner, as shown in Figure 17, which plots the
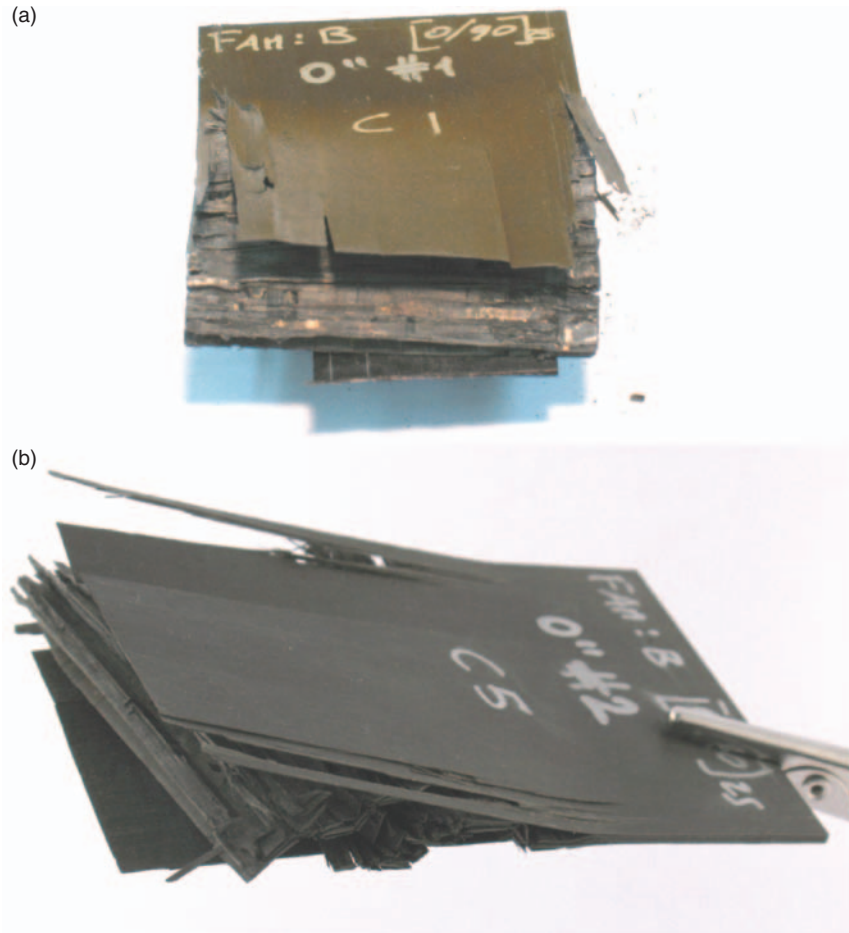
(a)

(b)



**Figure 13.** *(a, b) Crushed specimen at 0 in. (0 mm) unsupported height (same as original NASA fixture), material A, and steeple trigger.*

normalized values of load, total energy, and SEA against stroke and is relatively similar to Figure 12. Overall the crush is progressive and stable, and the failure mode is again a mixture of frond formation and fragmentation (Figure 18(a) and (b)), and similar tearing at the supports is visible.

Varying the unsupported height to 0.125 in. (3.2 mm) dramatically changes the observed behavior, as shown in Figure 19, and Figure 20(a) and (b). As in the case of material A, the failure morphology changes to that of a single delamination front, which forms at or near the mid-plane of the laminate and progresses smoothly during the crush. However, contrary to the case of material A, for material B, the load–displacement and SEA curves reach a stable plateau. The overall SEA is lower than in the case of the 0 in. (0 mm) unsupported height, where it exceeds 80 J/g, but still remains high around 65 J/g.

For unsupported heights of 0.25 and 0.5 in. (6.3 and 12.7 mm respectively) the trends observed are the same, with the exception of a couple of specimens that fail unstably due to localized buckling. This 'localized' buckling gives rise to the load–deflection curves of
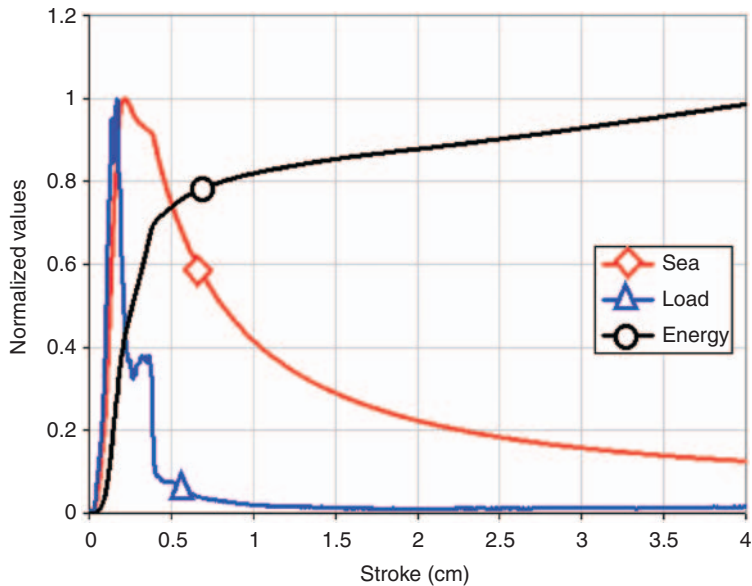
**Figure 14.** *Load, SEA, and total energy absorbed vs stroke at 0.125 in. (3.2 mm) unsupported height, material A, and notch or steeple trigger.*

Figure 21, where it is possible to see a rather unstable progression of the crush. This failure mode has the appearance of an accordion folding, whereby large segments of laminate snap unstably and fold over the already crushed portion of the laminate, Figure 22(a) and (b). The SEA measured for this type of failure mechanism is rather low, around 40 J/g, since large portions of the laminate remain intact and therefore do not contribute to dissipating energy.

For even greater unsupported heights, 0.75 in. and 1.0 in. (19 and 25.4 mm respectively), all specimens fail in this 'local' buckling fashion, and since even greater portions of the laminate remain intact, lower amounts of SEA are recorded. The curves and failure morphology are identical to those of Figures 21 and 22.

For material B, the trends reported can be summarized in Figures 16 and 23, which show the influence of unsupported height on the measured SEA. It can be seen that after an initial peak corresponding to the mixed failure mode of fragmentation and frond formation typical of the original NASA fixture, the values progressively drop with increasing unsupported height. For the saw-tooth trigger, they stabilize around an asymptotic value where stable crushing occurs by frond formation, before eventually dropping again once the specimen begins to fail by folding/local buckling.

Somewhat similar trends can be reported for the steeple trigger, as shown in Figure 16; however all SEA measured values appear to be shifted down by approximately 20 J/g. In the case of the steeple trigger, a true plateau is never reached, and it appears as if the SEA continues to decrease linearly with unsupported height. Although the failure morphology between the two triggers is observed to be the same, there appear to be unknown effects that lead to different values of SEA for the two trigger types. In particular, after the initial peak, the steeple trigger leads to a sharper drop before rising to reach a stable value, thus giving the resemblance of a trough in the load–displacement curve. These findings are
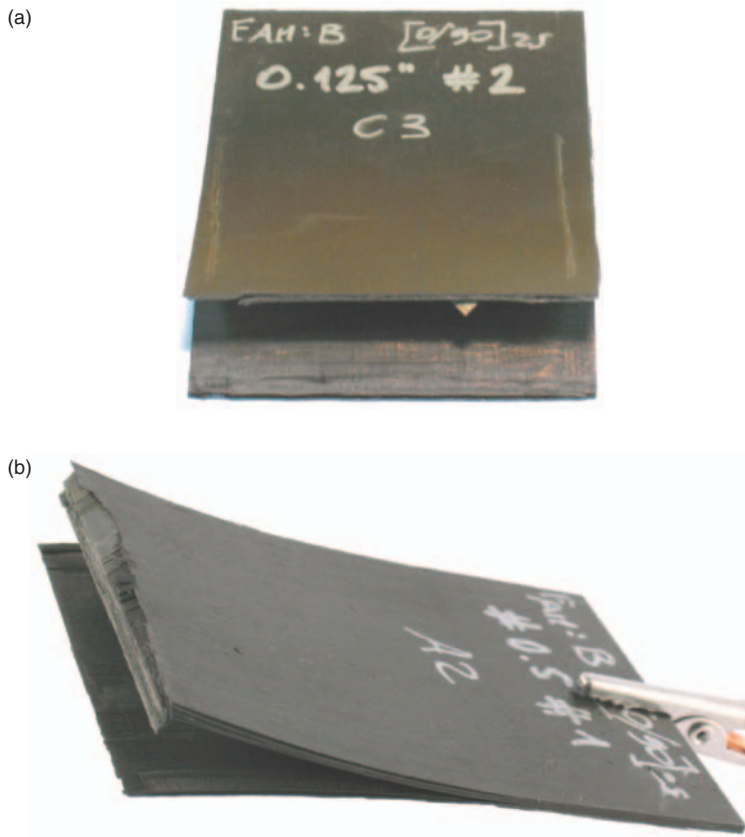
(a)



(b)



**Figure 15.** *(a, b) Crushed specimen at 0.5 in. (12.7 mm) unsupported height, material A and notch or steeple trigger.*
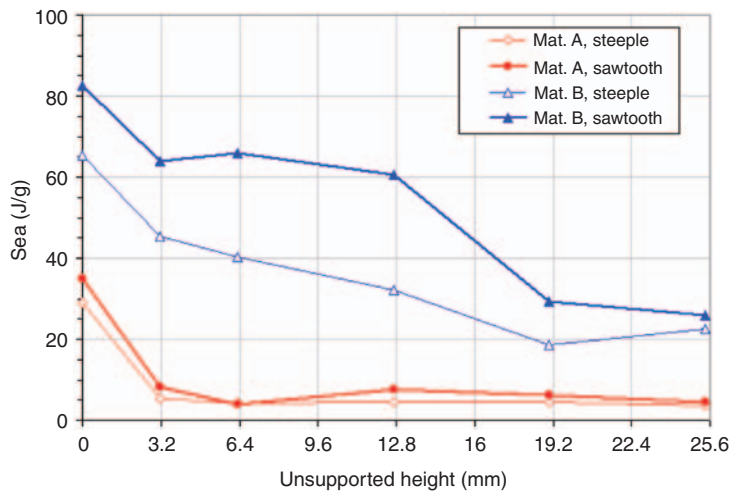


**Figure 16.** *Summary of all SEA average results as it varies with respect to unsupported height, for both materials and both trigger types.*
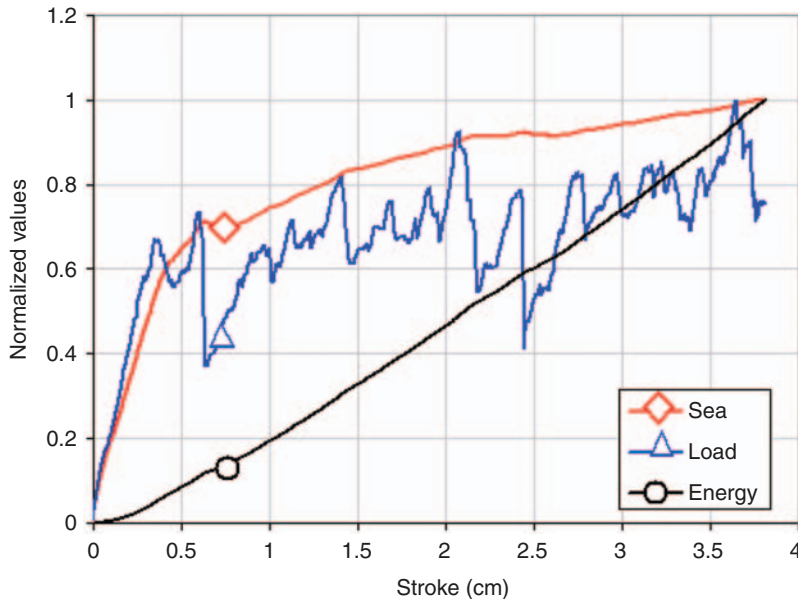
**Figure 17.** *Load, SEA, and total energy absorbed vs. stroke at 0 in. (0 mm) unsupported height (same as original NASA fixture), material B and notch or steeple trigger.*

however consistent with previous observations by other authors [6,17], but have never been fully explained.

## DISCUSSION

The modified test specimen/fixture combination appears to capture differences in measured SEA between material systems, based on their resistance to one specific failure mode (Figure 16). This crushing mode has been previously identified as lamina bending or splaying [2,3], as opposed to the fragmentation or transverse shearing mode, and it consists of the formation and propagation of a single delamination front, which leads to the formation of large fronds. For this type of failure mechanism, materials with higher interlaminar toughness absorb much greater energy than those with low interlaminar properties. Varying the resin type between material A and B has a dramatic influence on the load–deflection curves and SEA measurements. It should however be noted that materials A and B also differ in fiber type, since the T800 has greater modulus than the T700.

Steeple trigger appears to lead to lower SEA measurements, although the failure modes appear identical. Although preferable for its simplicity of manufacturing, for reasons analogous to those discussed by NASA [6,10–12] the steeple trigger is in general not recommended, while the saw-tooth trigger − similar to the NASA planar notch trigger − leads to more stable crush curves [17].

Using a non-zero unsupported height is fundamental to achieve stable failure by frond formation, and hence it is recommended to test the specimens in the range of 0.125–0.5 in. (3.2–12.7 mm). These values will vary depending on the stability of the specimen, and

(a)

(b)



**Figure 18.** *(a, b). Crushed specimen at 0 in. (0 mm) unsupported height (same as original NASA fixture), material B, and steeple trigger.*

hence on the section modulus. For material systems with lower elastic modulus or for thinner specimens, the optimum unsupported height values may be reduced, but for thicker or higher modulus systems they may be increased. For excessively large unsupported distances, there is the possibility to buckle specimens, and therefore to absorb low
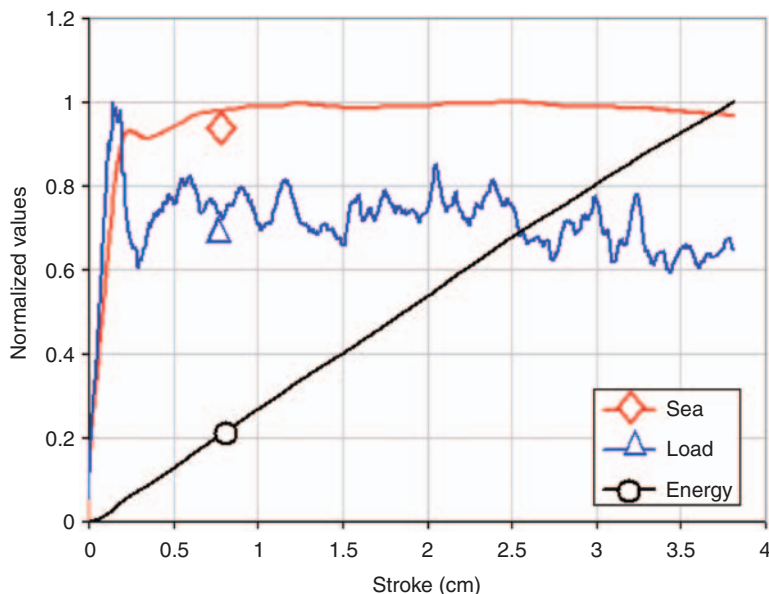
**Figure 19.** *Load, SEA, and total energy absorbed vs stroke at 0.125 in. (3.2 mm) unsupported height, stable crush, material B and notch trigger.*

amounts of energy. Employing a fully constrained specimen setup, with 0 in. (0 mm) unsupported height, leads to tearing of the laminate at the knife-edges, and to force formation of debris, which induce a combined failure mechanism of fragmentation and frond formation. This failure mode has been shown to yield much greater values of SEA than frond formation [2,3] but is not representative of a single failure mechanism.

In general, true crushing is not likely to ever be considered a failure mode, since it can manifest in four different forms [2]: fragmentation, frond formation, accordion folding (localized shell buckling), and macroscopic (or Euler) buckling. There is a potential therefore to develop a test method to capture a specific failure mode and the associated mechanisms by which energy is absorbed. In general, the stability of the specimen, hence its modulus and thickness, its compressive strength, and its interlaminar fracture toughness all participate in the race toward the selection of a natural preferred failure mode. If stability is not an issue, hence localized or global buckling is avoided, the key to favor fragmentation over frond formation is to suppress delamination propagation by using a corrugated or otherwise contoured specimen. On the other hand, if frond formation is the preferred or realistic failure mechanism, using a flat or otherwise minimally contoured specimen becomes critical to initiate frond formation. Results shown here are limited to laminated composites in tape prepreg form; hence further work needs to address different material forms such as discontinuous fibers and fabrics. Moreover, results need to be compared to other specimen shapes such as corrugated webs and tubular shapes.

In general, adoption of a self-supporting specimen, whether in the form of a corrugated web, a tube, or a channel section is preferable to that of a flat-plate-like specimen due to dependence and complexity of the anti-buckling fixture. The variability observed in the results, due to the inherent set-up of the fixture, may be overcome by adopting more complex support mechanisms, such as those mentioned in [17]. Currently, the choice of clamping a specimen against the knife-edges is subjective, and is a compromise between
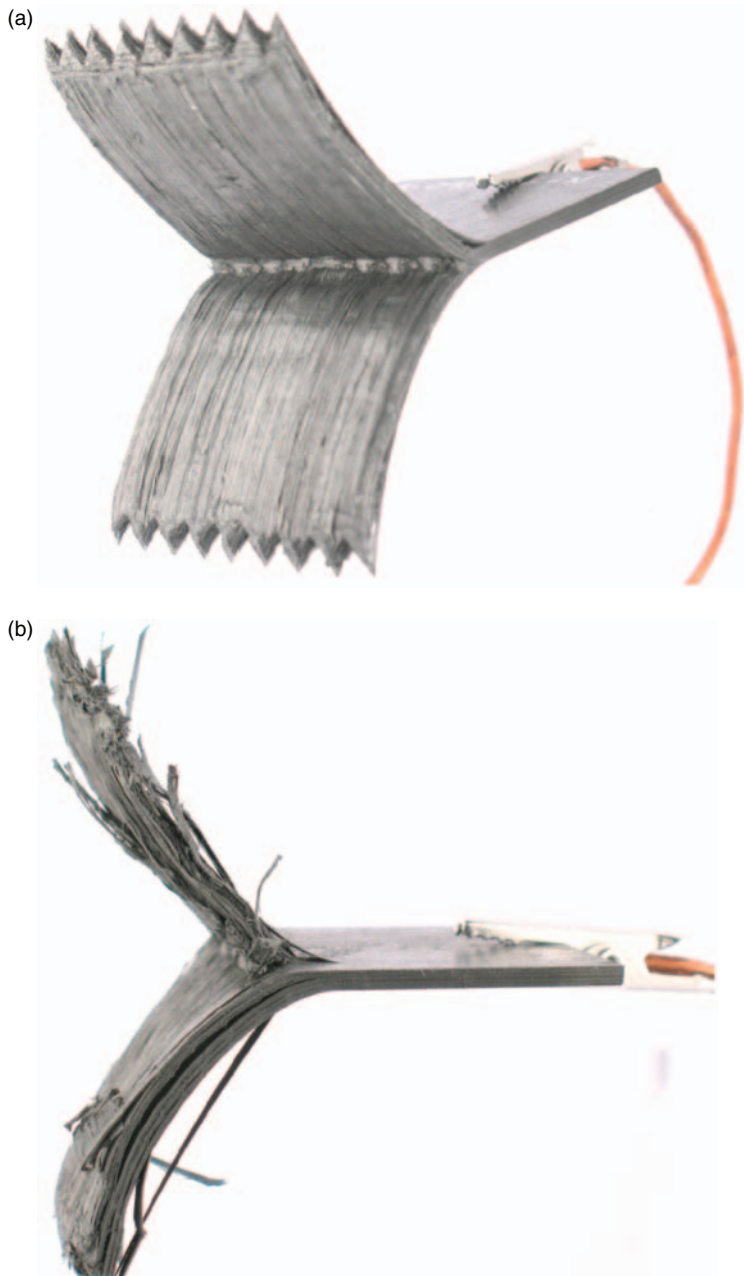
**Figure 20.** *(a, b) Crushed specimen at 0.125 in. (3.2 mm) of unsupported height, material B, and notch trigger.*

excessive clamping, which increases friction and hence energy absorption, and inefficient clamping, which then leads to unstable crushing and favors premature buckling. Furthermore, any attempt to model the crush phenomenon analytically, a difficult task for today's explicit finite element codes, is greatly hindered by the use of a support fixture,
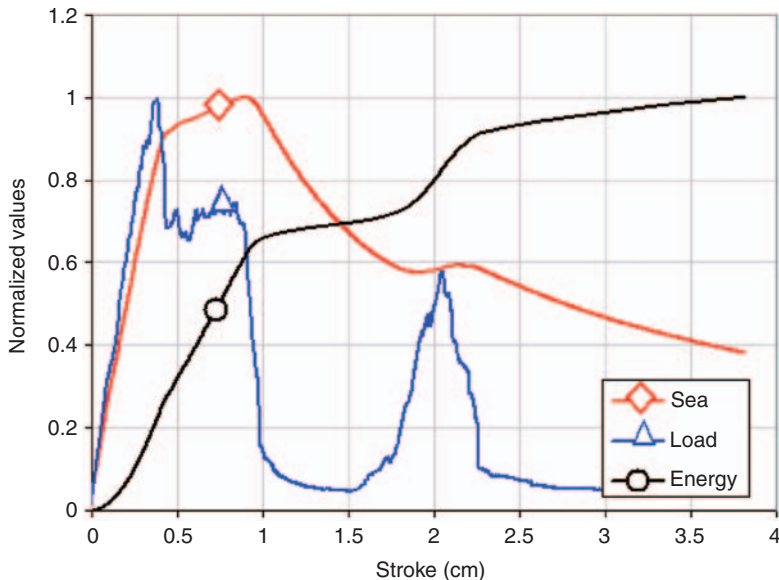
**Figure 21.** *Load, SEA, and total energy absorbed vs stroke at 0.25 in. (6.3 mm) unsupported height, unstable crush, material B and steeple trigger.*

whose interaction with the specimen is hard to characterize. Lastly, all tests discussed in this investigation are performed at quasi-static speeds, but there is a need to eventually transition to dynamic crushing to assess possible strain-rate-dependent failure character-istics of the materials. It could become even more difficult to employ a support fixture [19], due to the complexities associated with impacting the specimen only indirectly, and the need to adopt a self-supporting specimen could become even more significant.

It is fundamental for the composites community that a standard test method (or multi-ple) for composite crush energy absorption be developed, as there are currently no ways to compare material types, material forms, and lay-ups. However, the development of such standard will become possible only when the community accepts and embraces the fact that crushing is not a material property but a combined material/structure property.

## CONCLUSIONS

A specialized test fixture, based on a well-known NASA test fixture, was developed to measure composite crush energy absorption by means of flat-plate specimens. The fixture allows for modifying the degree of constraint of the specimen in proximity of the crush front by adjusting the unsupported height of the knife-edge supports, thus alleviating the problem of tearing at the edges and preventing the accumulation of debris in the proximity of the crush area. A systematic study was conducted to characterize the effect of the unsupported height on the measured energy absorption, which makes the task of assessing the true material behavior difficult. The fixture was used to characterize the effect of two prepreg tape material forms using two different trigger types, and it was found that dif-ferent combinations of these parameters lead to different crush behaviors. In conclusion, specimens that undergo what is traditionally referred to as crushing experience a

(a)

(b)

**Figure 22.** *(a, b) Crushed specimen at 0.25 in. (6.3 mm) of unsupported height, material B and steeple trigger.*
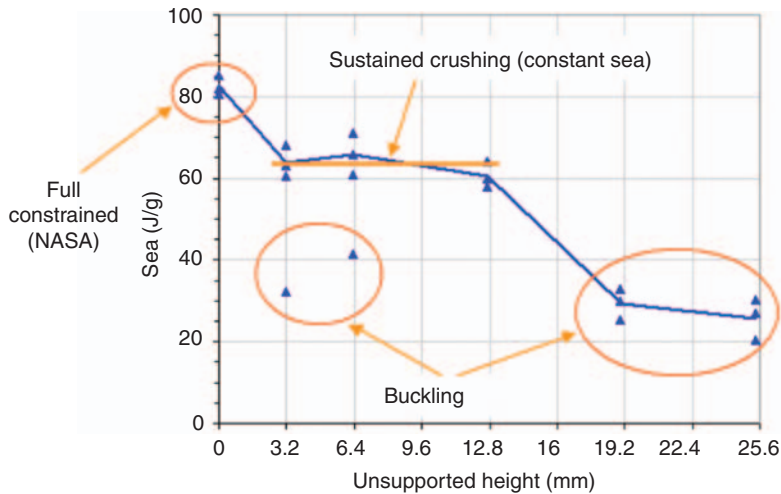
**Figure 23.** *Details from Figure 16 of SEA trend with unsupported height for material B, saw-tooth trigger only, showing individual test data points rather than average results.*

competition between various macroscopic failure modes, of which the prevailing one dictates the overall energy dissipation characteristics for the material/specimen/fixture combination.

## ACKNOWLEDGMENTS

## REFERENCES

1. Simula Technologies (2000). A Systems Approach to General Aviation Occupant Protection, NASA Langley Research Center Final Report, TR-00046.
2. Carruthers, J.J., Kettle, A.P. and Robinson, A.M. (1998). Energy Absorption Capability and Crashworthiness of Composite Material Structures: A Review, *Applied Mechanics Reviews*, **51**: 635–649.
3. Farley, G.L. and Jones, R.M. (1992). Crushing Characteristics of Continuous Fiber-reinforced Composite Tubes, *Journal of Composite Materials*, **26**(1): 37–50.
4. Jeryan, R. (2005). Energy Management Working Group Activities, In: *Proceedings of the 48th MIL-HDBK-17 Coordination Meeting – Crashworthiness Working Group*, Charlotte, NC, March 2005.

5. Nailadi, C. (2005). A Summary of the ACC Tube Testing Program, In: *Proceedings of the 49th MIL-HDBK-17 Coordination Meeting − Crashworthiness Working Group*, Santa Monica, CA, December 2005.

6. Jackson, K.E. (2005). Energy Absorption of Composite Materials and Structures, In: *Proceedings of the 49th MIL-HDBK-17 Coordination Meeting − Crashworthiness Working Group*, Santa Monica, CA, December 2005.

7. Wiggenraad, J.F.M. (2003). Crashworthiness Research at NLR: 1990−2003, NLR TP-2003-217, June 2003.

8. McCarthy, M.A., Harte, G.A., Wiggenraad, J.F.M., Michielsen, A.L.P.J., Kohlgrueber, D. and Kamoulakos, A. (2000). Finite Element Modeling of Crash Response of Composite Aerospace Sub-floor Structures, *Computational Mechanics*, **26**: 250−258.

9. "Crashworthiness and Energy Management," *Composite Materials Handbook (CMH-17)*, Vol. 3, Chap. 13, Rev. G.

10. Lavoie, J.A. and Morton, J. (1993). Design and Application of a Quasistatic Crush Test Fixture for Investigating Scale Effects in Energy Absorbing Composite Plates, NASA CR 4526, July 1993.

11. Jackson, K., Morton, J., Lavoie, J. and Boitnott, R. (1994). Scaling of Energy Absorbing Composite Plates, *Journal of the AHS*, **39**(1): 17−23.

12. Lavoie, J.A. and Kellas, S. (1996). Dynamic Crush Tests of Energy-absorbing Laminated Composite Plates, *Composites Part A*, **27**(6): 467−475.

13. Johnson, A. (2006). Determination of Composite Energy Absorption Properties, In: *Proceedings of the 50th MIL-HDBK-17 Coordination Meeting − Crashworthiness Working Group*, Chicago, IL.

14. Daniel, L., Hogg, P.J. and Curtis, P.T. (1999). The Relative Effects of Through-thickness Properties and Fibre Orientation on Energy Absorption by Continuous Fibre Composites, *Composites Part B*, **30**: 257−266.

15. Cauchi Savona, S. and Hogg, P.J. (2006). Investigation of Plate Geometry on the Crushing of Flat Composite Plates, *Composites Science and Technology*, **66**(11−12): 1639−1650.

16. Barnes, G. (2005). Composite Crush Coupon Testing, In: *Proceedings of the 49th MIL-HDBK-17 Coordination Meeting − Crashworthiness Working Group*, Santa Monica, CA.

17. Bolukbasi, A.O. and Laananen, D.H. (1995). Energy Absorption in Composite Stiffeners, *Composites*, **26**(4): 291−301.

18. Feraboli, P. (2008). Development of a Corrugated Test Specimen for Composite Materials Energy Absorption, *Journal of Composite Materials*, **42**(3): 229−256.

19. Lavoie, J.A., Morton, J., Kellas, S. and Jackson, K. (1994). New Test Method for Measuring Static and Dynamic Energy Absorption Capacity of Composite Plates, In: Visconti, C. (ed.), *Advancing with Composites*, Vol 2, **3rd edn**, pp. 239−250, Design and Applications, Milan, Italy.